Journal of Engineering Science and Technology Review 14 (2) (2021) 184 - 191

JOURNAL OF
**Engineering Science and Technology Review**

www.jestr.org

Research Article

# Influence of Coal Failure Characteristics on Gas Occurrence States

**Chuanqi Zhu* and Shaobo Li**

*State Key Laboratory of Mining Response and Disaster Prevention and Control in Deep Coal Mines, Anhui University of Science and Technology, Huainan, Anhui 232001, China*

Received 18 January 2021; Accepted 31 March 2021

***Abstract***

A sudden change of gas occurrence states can easily trigger coal and gas dynamic disasters. However, determining the change laws of gas occurrence states on the working face of high gassy coal seams is difficult. The coal failure characteristics have a direct effect on gas occurrence states. Under the engineering background of the 11518 fully mechanized coal mining face of Panyi Mine in Huainan Coal Mining Area in China, the coal mining-induced stress, ultrasonic wave velocity, gas pressure, and gas flow at different positions in front of this working face were first measured. A stress meter, an acoustic wave-monitoring analyzer, a gas pressure determinator, and a gas flow monitor were used to analyze the gas occurrence states and change laws from the angle of coal failure characteristics. Next, the change laws of gas occurrence states in the coal masses with different failure degrees were investigated. Afterward, the evolutionary mechanism of gas pressure was theoretically analyzed via the theory of equation of gas state. Results show that the coal mining-induced stress, gas pressure, and gas flow are first steady, then increase, and gradually reduce with the advancement of the working face. Meanwhile, the ultrasonic wave velocity is steady, reduces, and then becomes steady again. The coal mass in front of the working face can be divided into intense damage zone, damage zone, and slight damage zone from the rib to the coal seam strike at the outer edge. The gas pressure of coal mass is the highest in the damage zone. Gas treatment measures implemented by the field technicians in the damage zone can effectively improve the gas occurrence states and prevent and control the coal and gas dynamic disasters. The obtained conclusions have enriched the theoretical understanding of gas occurrence states and can provide a basis for reducing gas accidents.

*Keywords:* High gassy coal seams, Ultrasonic wave velocity, Failure characteristics, Mining-induced stress, Gas occurrence states

## 1. Introduction

Underground mining is the main means of coal resource mining in the globe. In the major coal resource mining countries, such as Australia, Russia, India, and China, with complicated underground coal seam occurrence conditions, the mining disturbance will probably induce all types of safety accidents [1 - 4]. The coal and gas dynamic disasters are regarded as the main type of coal mine accident. In recent years, the mining depth of global coal resources is gradually increasing with the depletion of shallow coal resources. The gas pressure of coal seam, gas content, in-situ stress, and gas emission are increasing, while the coal permeability is gradually decreasing. The number of outburst coal seams is increasing, and the risk of coal and gas dynamic disasters is increasing. The coal and gas dynamic disasters once took place during the mining of Metropolitan Coal Mine and Tahmoor Coal Mine in Australia, Sanjia Coal Mine, Didao Shenghe Coal Mine, and Xingyu Coal Mine in China. According to the incomplete statistics, 878 coal and gas power accidents occurred in 22 mining areas in Australia, especially during high gas coal mining, which is more prone to sudden gas accidents. Coal and gas power disasters cause a large number of casualties, which can bring huge economic losses and cause bad social impact [5, 6].

Many scientific researchers and field technicians have been extensively exploring for a long time to prevent and control coal and gas dynamic disasters. In view of high gas coal seam, based on the idea of changing the gas occurrence state of the coal body, several field prevention and control measures have been proposed from the perspective of reducing gas content and gas pressure. On this basis, the key coal and gas dynamic disaster governance technology of “extraction first, mining second” is formed and has been successfully used in some mining areas with good effects; thus, the occurrence frequency of coal and gas dynamic disasters is greatly reduced [7 - 9]. In the present prevention and control of coal and gas dynamic disasters, treatment measures are mostly taken for the coal seam on the whole mining working face. The technical effect of global prevention and control on the coal seam of the whole working face is satisfying; however, the engineering quantities are large, high material and labor cost, and low implementation efficiency. By contrast, the regional prevention and control technology that adopts coal and gas dynamic disaster control measures was more efficient and economic in the location where coal and gas dynamic disasters are prone to sudden occurrence. Nevertheless, the field application of regional prevention and control technology for coal and gas dynamic disasters lacks mature theoretical guidance.

The change of gas occurrence states is one of the key factors triggering the coal and gas dynamic disasters [10]. Before the recovery of high gassy coal seams, the beforehand gas extraction measure is already taken. After

*E-mail address: zhuchuanqi2013@126.com
ISSN: 1791-2377 
doi:10.25103/jestr.142.22

the formation of coal mining face, the gas content and pressure in the coal body are low, and the gas is in a dynamic equilibrium state. The gas occurrence state at different locations from the working face is relatively stable. Hence, coal and gas dynamic disasters may not easily occur. Under the action of mining-induced stress during the coal seam recovery process, the gas flow is aggregated; thus, the occurrence state is extremely unstable, thus leading to sudden coal and gas dynamic disasters. The key to efficient prevention and control of dynamic disasters lies in taking effective gas treatment measures in the region prone to coal and gas dynamic disasters. Determining the gas occurrence states and its change laws in front of the working face during the recovery period of high gassy coal seams and identifying the zones with dangerous risks of coal and gas dynamic disasters will be of great engineering practical significance.

## 2. State of the art

In the mining of high gas coal seam, it is the basis and premise for accurately obtaining the change rule of gas occurrence state and determining the prone area of dynamic disasters, which effectively implementing the prevention and control measures of coal and gas dynamic disasters. Experts and scholars have carried out a large number of studies on the variation law of gas occurrence state in coal seams through theoretical model analysis, numerical calculation, and field measurement to study the change law of gas occurrence state in different regions during coal seam mining. The study mainly includes the gas occurrence state at different positions of mining face and the influence of mining depth, internal structure, permeability, mining disturbance, and temperature on the gas occurrence state.

With regard to the gas occurrence states in different areas, Sobczyk et al. [11] acquired the change laws of gas pressures at different positions of a coal seam during the occurrence of a gas disaster through a laboratory experiment on coal and gas outbursts. Alekseev et al. [12] analyzed the elastic energy of a gas-containing coal mass and acquired the gas pressure distribution characteristics in the coal seam, thus providing a theoretical basis for predicting the gas dynamic disasters. Adel et al. [13] used Comsol numerical calculation software to simulate the change laws of gas pressure and flow in the gas extraction process taking Tabas and Shahrood basin coal mines as the study objects. Si et al. [14] measured the gas pressure and flow laws in the goaf during the recovery process of a working face in an Australian mining area. Ripepi et al. [15] determined the gas content distribution characteristics in a coal field in the middle of Appalachia via a new gas content determination method. Lin et al. [16] established a stress field, seepage field, and diffusion field coupling model to probe into the distribution characteristics of gas pressure in the matrix and gas pressure in cracks along the coal seam strike during the extraction. Wang et al. [17] conducted a simulation study of the dynamic distribution characteristics of gas pressure in front of a coal roadway via the LBM numerical software. Ma [18] explored the 3D distribution characteristics of gas pressure under mining impact through the field test and theoretical analysis. In terms of the influence laws of different factors on the gas occurrence states, Scott et al. [19] discussed about the relationship between gas pressure and burial depth of coal seam according to measured data. Directing at anthracitic coal in Qinshui Coal Field of China, Si et al. [20] explored the influences of pore structure and shattered state of coal mass on the change laws of gas pressure during the extraction. Jing et al. [21] used the matrix theory to characterize the grid distribution of coal mass and discussed the relationship between gas flow laws and permeability. Specific to the coal mass in Donets Basin, UI'yanova et al. [22] studied the influences of metamorphic grade and macro–meso internal structure of coal mass on the gas content. Kozyreva et al. [23] investigated the influences of the pressure of added gas on the gas occurrence and flow laws in the coal mass of Kuznetsk Basin by adding helium. Duan et al. [24] discussed the influence of the initial permeability anisotropy ratio on the gas pressure distribution in the coal seam during the gas extraction on the basis of the permeability model. Xie et al. [25] analyzed the coupling effect between gas pressure and mining-induced stress on the basis of the measured data of mining-induced stress and gas pressure in the coal seam recovery process. Wei et al. [26] studied the relationship between gas pressure and coal seam temperature through the heat–fluid–solid coupling model of gas transport. Scholars have basically reached a consensus over the gas occurrence states at different positions of the mining working face through studies. However, the factors influencing the change laws of gas occurrence states are not completely investigated yet.

During coal seam mining, mining disturbance causes coal deformation, destruction, and even movement. The gas in the coal body during coal failure is bound to continue to diffuse, flow, and gather, and the gas occurrence state continues to dynamically change. The failure characteristics of coal directly determine the occurrence of gas. The coal failure characteristics directly decide the gas occurrence states; thus, the influencing laws of coal failure characteristics on the gas occurrence states must be studied to provide a theoretical basis for revealing the evolutionary mechanism of gas occurrence states and preventing and controlling coal and gas dynamic disasters. On this basis, this study takes the 11518 fully mechanized mining face of Panyi Coal Mine in Huainan Mining Area of China as the background. Moreover, this study uses the ultrasonic wave velocity to characterize the failure characteristics of coal body. Furthermore, this work studies the variation law of coal mining stress, ultrasonic wave velocity of coal, gas pressure, and gas flow during the mining process of working face through field measurement. This study also analyzes the relationship between coal failure characteristics and gas occurrence state and explores the evolution mechanism of gas pressure distribution characteristics.

The remainder of this study is organized as follows. Section 2 introduces the research status regarding the gas occurrence states in coal seams. Section 3 presents a concrete field measurement scheme. Section 4 analyzes the measurement results of mining-induced stress, failure characteristics, gas pressure, and gas flow in coal mass and explores the relationship between gas occurrence states and coal failure characteristics. This section also reveals the evolutionary mechanism of gas pressure and probes into the key zones needing prevention and control of coal and gas dynamic disasters. Section 5 draws the conclusions.

## 3. Methodology

### 3.1 Geological and mining technical conditions of the working face

The elevation and average tilt length of 11518 fully mechanized coal mining face of Panyi Coal Mine in Huainai

Coal Mining Area, China are −576.7 to −598.5 and 202 m, respectively. This working face is located in the coal mining area of east no. 1 B formation. The east area includes east no. 2 −530 to −790 m 6-1 rail rise in coal floor, east no. 2 −530 to −790 m 6-1 return air rise in coal floor, and east no. 2 −530 m system roadway. The south area includes east no. 2 −530 m system roadway and 11618 high-level gas drainage roadway. The west area includes east no. 1 B formation coal system roadway and east no. 1 4-1 return air downhill in the coal floor. The north area includes the 21118 and 11318 working faces. The upper part corresponds to the already recovered 13-1 and 11-2 coal seams, 11518 high-level gas drainage roadway in the haulage roadway, 11518 upper high-level gas drainage roadway in the return air roadway, and 11518 high-level gas drainage roadway of the cut eye. The layout of the main roadways on the working face is shown in Fig. 1.

The 11518 fully mechanized coal mining face has stable coal seam occurrence, where the thickness of coal seam ranges from 0.7 m to 3.8 m (average thickness: 2.2 m), and the average dip angle is 7°. At the coal seam, the original gas pressure is 2.3 MPa, and the original gas content is 7.38 $m^3 \cdot t^{-1}$. The gas emissions from the adjacent coal seams, such as the underlying 7-1, 6-1, 5-2, 5-1, 4-2, and 4-1 coal seams, are illustrated in Table 1. The relative and absolute gas emissions on the working face are 10.8 $m^3 \cdot t^{-1}$ and 38 $m^3 \cdot min^{-1}$, respectively, during the recovery period. The mechanical ventilation is U-shaped, the return air volume is 2.040 $m^3 \cdot min^{-1}$, and windblown gas emission is 10.2 $m^3 \cdot min^{-1}$, which accounts for 26.8% of the total gas emission. Meanwhile, two-roadway bedding borehole extraction, extraction of high-level gas drainage roadway in the upper ventilating roadway, extraction of the high-level gas drainage roadway in the lower crossheading, extraction of the goaf by buried pipes, trans-strata borehole extraction along the floor strike of the upper and lower ventilating roadways, and other gas control measures are taken. The amount of gas extracted is 27.8 $m^3 \cdot min^{-1}$, and the gas extraction rate is 73.2%. After the beforehand gas extraction measure is taken, the residual gas content, residual gas pressure, and resolvable gas content of the working face are 4.52 $m^3 \cdot t^{-1}$, 0.22 MPa, and 3.7 $m^3 \cdot t^{-1}$, respectively.

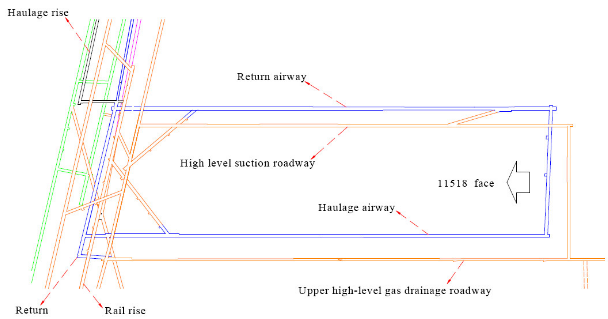

**Fig. 1.** Layout plan of main roadways on the 11518 working face

**Table. 1.** Gas emissions in the adjacent coal seams on the working face

| Coal | Average thickness (*m*) | Spacing (*m*) | Original gas content ( $m^3 \cdot t^{-1}$) | Gas discharge rate of the adjacent coal seams (%) | Gas emission from adjacent coal seam ( $m^3 \cdot t^{-1}$) |
|---|---|---|---|---|---|
| 7-1 | 2.15 | 14.62 | 8.05 | 35.4 | 2.2 |
| 6-1 | 3.00 | 27.89 | 8.6 | 9.9 | 0.4 |
| 5-2 | 1.61 | 41.36 | 8.7 | 7.0 | 0.42 |
| 5-1 | 1.16 | 45.35 | 8.7 | 4.7 | 0.13 |
| 4-2 | 1.69 | 53.15 | 9.22 | 5.2 | 0.51 |
| 4-1 | 3.34 | 58.09 | 11.1 | 5.7 | 0.68 |
| Total | | | | | 4.34 |

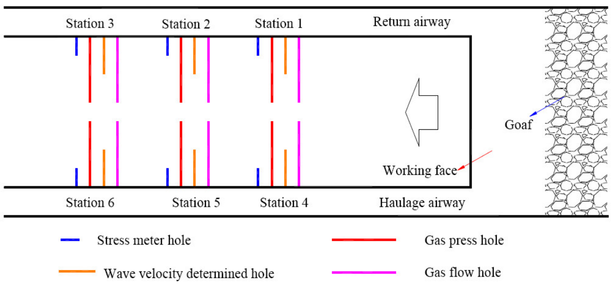

**Fig. 2.** Layout plan of the monitoring equipment on the working face

### 3.2 Field measurement scheme

The change laws of mining-induced stress, ultrasonic wave velocity, gas pressure, and gas flow in the coal seam were mainly monitored on the field. The concrete testing scheme was as follows. An observation station was arranged in each of the return air roadway and haulage roadway at 200, 250, and 300 m away from the working face. Each observation station was arranged with stress observation hole, ultrasonic wave velocity observation hole, gas pressure observation hole, and gas flow observation hole, the depths of which were 10, 20, 30 and 30 m, respectively. The hole spacing was 5 m. The stress meter, acoustic wave monitoring analyzer, gas pressure determinator, and gas flow monitor were installed in the four holes to determine the mining-induced stress, ultrasonic wave velocity, gas pressure, and gas flow (Fig. 2).

## 4 Result Analysis and Discussion

### 4.1 Distribution laws of mining-induced stress

Fig. 3 is the variation tendency chart of the mining-induced stresses at return air and haulage roadway sides along the coal seam strike under different advancement distances of the working face. The analysis showed that the mining-induced stress at the return air roadway side along the coal seam strike was stabilized at approximately 7.2 MPa in the area beyond 40 m range from the working face. The mining-induced stress was first slowly increased, rocketed, and considerably reduced within 40 m range from the working face with the advancement of the working face. Specifically, the mining-induced stress first slowly increased from 7.2 MPa at 40 m from the working face to 9.5 MPa at approximately 26 m from the working face (by 2.3 MPa). Afterward, the mining-induced stress sharply increased to 23 MPa at approximately 9 m from the working face, with the increased amplitude reaching 142%, and reached the maximum value at this position. Finally, the mining-induced stress rapidly reduced from the peak point until reaching zero at the rib.

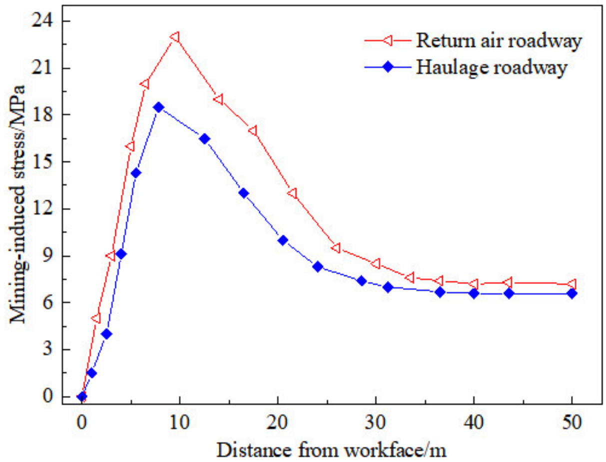


**Fig. 3.** Variation tendency chart of mining-induced stress

The change laws of the mining-induced stress at the haulage roadway side along the coal seam strike were identical with those at the return air roadway side. When the working face was advanced to 28 m from the observation point, the mining-induced stress was significantly increased; at 8 m position from the working face, it reached the extremum 18.5 MPa; it was rapidly reduced within 8 m range from the working face. The peak value of mining-induced stress at the return air roadway side was slightly larger than that at the haulage roadway side, and the peak area was also slightly ahead of that at the haulage roadway side.

### 4.2 Gas pressure distribution characteristics

Fig. 4 shows the variation tendency chart of gas pressure at the return air and haulage roadway sides along the coal seam strike under different advancement distances of the working face. The gas pressure at the return air roadway side along the coal seam strike was basically stabilized at the residual pressure of 0.22 MPa in the area beyond approximately 40 m from the working face. The gas pressure was elevated within approximately 30 – 40 m from the working face with the advancement of the working face. This factor was remarkably increased within approximately 15 – 30 m from the working face. At 15 m from the working face, gas pressure reached the maximum value of 0.41 MPa. During this process, the gas pressure was increased by 0.011 MPa every time the working face was advanced for 1 m. Thereafter, the gas pressure was rapidly reduced within the 15 m range from the working face until reaching zero at the rib.

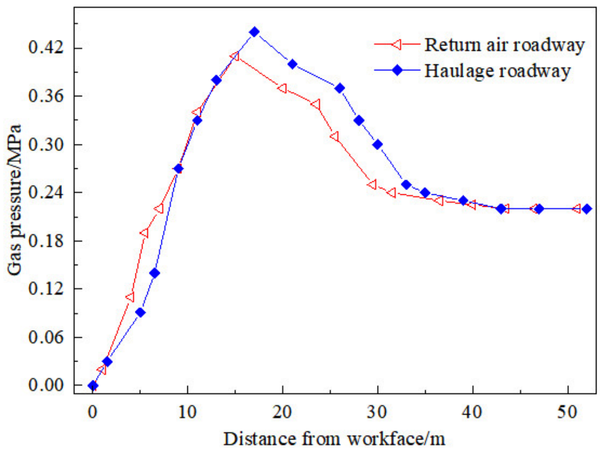


**Fig. 4.** Variation tendency chart of gas pressure

The gas pressure at the haulage roadway side along the coal seam strike was also first steady, subsequently increased, then declined, and finally reached the peak value of 0.44 MPa at approximately 17 m in front of the working face with the advancement of the working face. The peak gas pressure at the haulage roadway side was slightly higher than that at the return air roadway side. The peak area was also slightly ahead of that at the return air roadway side, and the gas pressure increased from 0.22 MPa after the beforehand extraction to 0.44 MPa during the coal seam recovery process, indicating the aggravated risk of the coal and gas outburst disasters.

### 4.3 Change laws of gas flow

The variation tendency chart of the gas flows at the return air roadway side and haulage roadway side along the coal seam strike under different advancement distances of the working face is displayed in Fig. 5. The gas flow at the return air roadway side was stabilized at approximately 0.10 $m^3 \cdot min^{-1}$ within the area 20 m from the working face. This flow was gradually increased within approximately 20 – 7 m from the working face, which was continuously advanced. The peak value is 0.24 $m^3 \cdot min^{-1}$ when it is approximately 7 m in front of the working face, and then it significantly decreases to zero. With the working face approaching, the variation law of coal gas flow in the transport roadway side along the coal seam strike is the same as that in the return air roadway side. The maximum value (0.21 $m^3 \cdot min^{-1}$ ) appeared at approximately 6 m in front of the working face, and the gas flow at the return air roadway side was generally larger than that at the haulage roadway side.

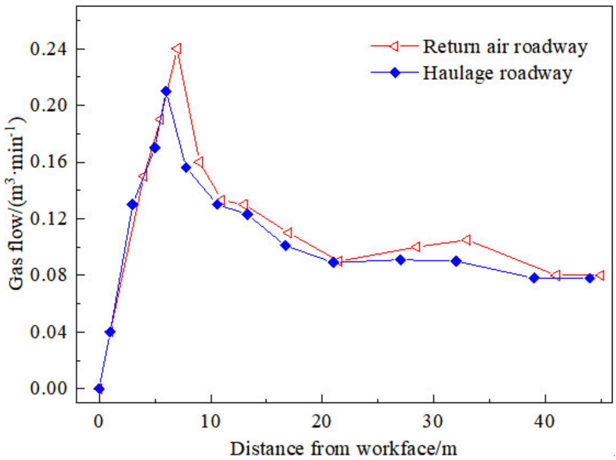


**Fig. 5.** Variation tendency chart of gas flow

Under the influence of mining disturbance, the variation law of coal gas pressure, gas flow, and mining stress in the side of return airway and transport roadway along the coal seam is basically the same. The trend is first stable, then increases, and finally decreases with the advancement of the working face. However, the distribution range of the peak area is different. The peak area of gas pressure was ahead of that of mining-induced stress whether at the return air or haulage roadway side. The peak area of gas pressure basically corresponded to the area with the rapid increase in mining-induced stress. By contrast, the peak area of mining-induced stress was slightly ahead of that of gas flow under both circumstances.

### 4.4 Change laws of ultrasonic wave velocity

Fig. 6 is the variation tendency chart of ultrasonic wave velocity at the return air and haulage roadway sides along the coal seam strike under different advancement distances of the working face. The ultrasonic wave velocity at the return air roadway side was first steady, subsequently reduced, and then steady again with the advancement of the working face. It was kept at 240 $m\cdot s^{-1}$ in the area approximately 30 m from the working face. The wave velocity was slowed down within 5–30 m range from the working face. This factor first gradually declined from 247 $m\cdot s^{-1}$ at 30 m to 47 $m\cdot s^{-1}$ at 5 m and was then stabilized at 47 $m\cdot s^{-1}$. The variation trend of ultrasonic wave velocity at the haulage roadway side was identical with that at the return air roadway side, and the area with declining wave velocity was within approximately 30–6 m from the working face.

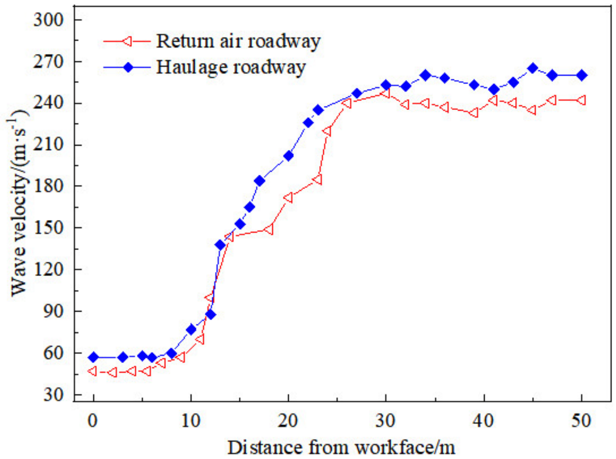


**Fig. 6.** Variation tendency chart of the ultrasonic wave velocity in coal mass

### 4.5 Gas pressure distribution and gas flow laws in coal masses with different failure degrees

According to the variation of the ultrasonic wave velocity of the coal body under different advancing distances, the coal body in front of the work is divided into severe areas from the coal wall to the outer coal seam, including damage area I, damage area II, and mild damage area III (Fig. 7).

Intense damage zone (I): The coal mass in this zone was under the post-peak failure state after the action of high mining-induced stress with weak bearing capacity. Mining stress is low, and the ultrasonic wave velocity has been stable at a low value. The fully developed macroscopic cracks in the coal body provide a smooth channel for gas flow. The free gas in the coal body quickly releases to the working face and the two lanes, and the adsorbed gas continuously converts to the free gas. The gas pressure is low, and the gas flow rapidly increases with the distance from the working face. The adsorbed gas were continuously transformed into porous medium-confined gas, the gas pressure was low, and the gas flow was rapidly enlarged with the advancement of the working face.

Damage zone (II): The stress release of coal mass in the intense damage zone was transferred outward. Then, a high stress zone was formed, and the coal mass suffered a certain damage in the damage zone under strong bearing state. The mining-induced stress was high, and the ultrasonic wave velocity was gradually accelerated with the increase in distance. A large number of microcracks are present in the coal body, the volume of the coal body expands, and the expansion phenomenon occurs. A large amount of gas is desorbed on the surface of the crack, and the free gas increases. The micro cracks in the coal body have not been aggregated and penetrated. In this zone, which was basically overlapped with the mining-induced dilation zone of the coal mass, a confined space could be formed without a gas flow channel with the adjacent zone. Without mutual flow, the gas flow was reduced, and the desorbed gas was gathered in this zone. Accordingly, the gas pressure reached the maximum.

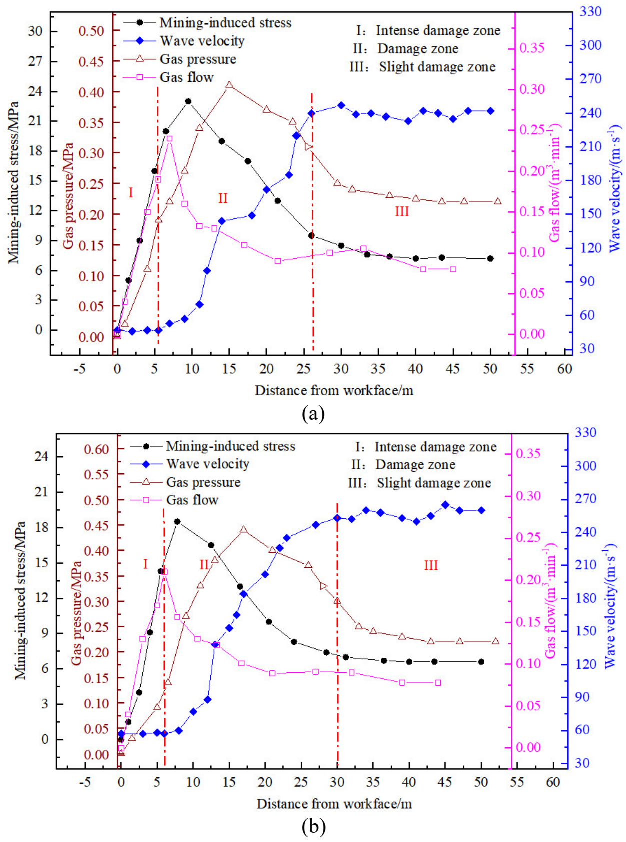


**Fig. 7.** (a) Variation tendency chart of mining-induced stress, gas pressure distribution, and gas flow in coal masses with different failure degrees at the return air roadway side. (b) Variation tendency chart of mining-induced stress, gas pressure distribution, and gas flow in coal masses with different failure degrees at the haulage roadway side

Slight damage zone (III): The coal mass in this zone was influenced by the mining disturbance to a small extent; it was under the original intact state with the strongest bearing capacity; however, the external load that it bore was small. The mining dynamic stress is low, and the velocity of ultrasonic wave has been stable at a large value. The adsorbed gas and free gas in the coal body are in a dynamic equilibrium state. The gas pressure gradually decreases to a low value outward from the rib on the working face, and the measured gas flow was low.

The gas occurrence states are associated with the coal failure characteristics, and both are regular to a certain extent. The gas pressure was low in the coal mass in the intense damage zone, and that in the damage zone was slightly increased. Meanwhile, the gas pressure in the slight damage zone was gradually reduced to a low value outward from the working face.

### 4.6 Evolutionary mechanism of gas pressure

Under the action of mining-induced stress, the cracks were continuously developed and extended in the coal mass. The failure degree was continuously elevated, the physical and mechanical characteristics were considerably changed, the porosity of coal mass was changed, and gases were observed in the coal mass. The gas pressure also continuously evolved. The theoretical relationship between gas pressure and its basic dependent variables should be established to investigate the evolutionary mechanism of gas pressure. In accordance with the equation of gas state, the gas pressure $p$ of coal mass during the mining process can be expressed as [27]

$$p = \frac{X_y T' p_0 \xi}{r T_0} \tag{1}$$

where $X_y$, $r$, $p_0$, $T_0$, $T'$ and $\xi$ are porous medium-confined gas content in the coal mass, pore volume of coal mass with unit weight, pressure under standard state, absolute temperature under standard state, absolute temperature of gas, and coefficient of gas compressibility, respectively. The pore volume of coal mass with unit weight $r$ can be solved through the following equation:

$$r = \frac{f'}{\rho'} \tag{2}$$

where $f'$ is porosity of coal mass, and $\rho'$ is the apparent density of coal mass.

Gas pressure $p$ can be solved through the combination of Eqs. (1) and (2):

$$p = \frac{\rho' X_y T p_0 \xi}{f' T_0} \tag{3}$$

From Eq. (3), the gas pressure of coal mass is mainly controlled by two basic variables—porous medium-confined gas content $X_y$ and porosity $f'$—during the recovery process. The gas pressure is positively correlated with the porous medium-confined gas content while being inversely proportional to the porosity. Fig. 8 displays the relationships of gas pressure $p$ of coal mass with porous medium-confined gas content $X_y$ and porosity $f'$.

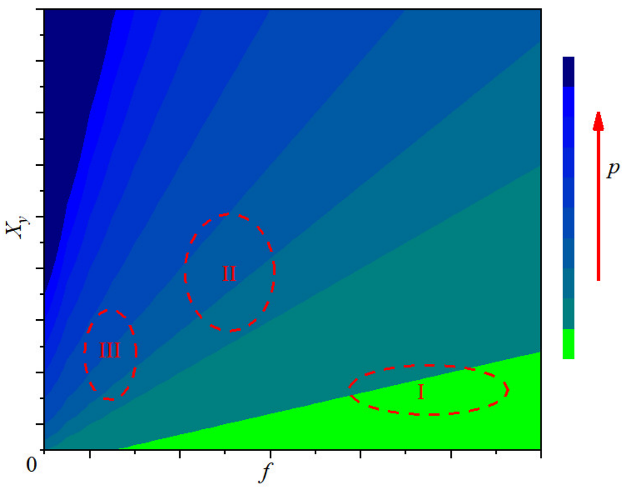


I: Intense damage zone; II: Damage zone; III: Slight damage zone
**Fig. 8.** Schematic of relationships of $p$ with $X_y$ and $f'$ of coal masses with different damage degrees

In the intense damage zone, several local macrocracks in the coal mass were gathered to form one or multiple through macroplanes after being extended along the weak path, $f'$ reached the maximum, the gas flow was unblocked, $X_y$ was reduced, and the gas pressure experienced a remarkable drop.

In the damaged zone, the internal microcracks of the coal began to crack and expand after closing. Meanwhile, many microcracks were initiated, and $f'$ was slightly larger than that in the slightly damaged area. Nevertheless, a large amount of gas was desorbed on the surface of the internal cracks of the coal in this area, $X_y$ was greatly increased, and gas pressure $p$ reached the maximum value.

In the slight damage zone, the internal microcracks in the coal mass were gradually compressed and closed. Accordingly, porosity $f'$ reached the minimum value, and the desorbed gas and porous medium-confined gas were under dynamic equilibrium in the coal mass. The free gas content $X_y$ was unchanged. Gas pressure $p$ was increased to a small extent with the reduction in porosity; however, it was still low.

### 4.7 Key area needing prevention and control of coal and gas dynamic disasters

The mining disturbance broke through the original equilibrium of gas occurrence states and resulted in the gas release, transfer, and redistribution. The change laws of gas occurrence states directly decided the risk degree of coal and gas dynamic disasters. According to the correlation and regularity between the gas occurrence state and the damage failure characteristics of coal body, a large number of microcracks were produced in the coal body in the damage area, and the free gas accumulates in the microcracks. The gas pressure of the coal body in the confined space was the highest, and the basic corresponding mining stress rapidly increased. The elastic potential of coal accumulation was the largest. The elastic energy gathered in the coal mass was the maximum; if it was suddenly released, it could easily trigger coal and gas dynamic disasters. Accordingly, the damage zone was a key area for disaster prevention and control (Fig. 9). Therefore, gas treatment measures, if implemented by field technicians in the damage zone, can effectively prevent and control coal and gas dynamic disasters.

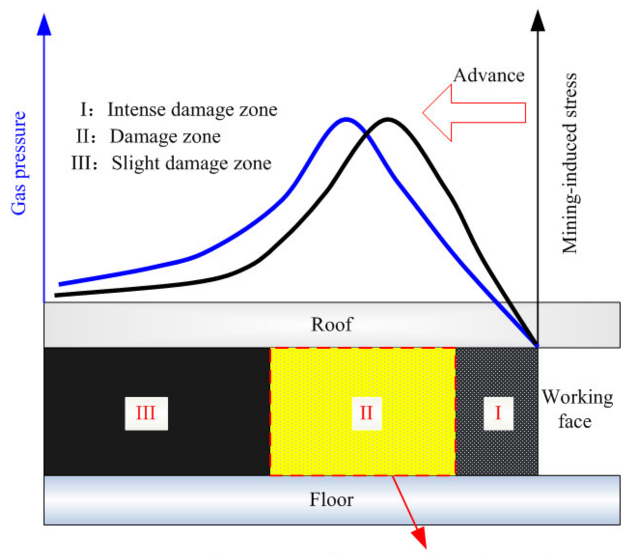


**Fig. 9.** Key areas needing prevention and control of coal and gas dynamic disasters (schematic)

## 5. Conclusions

The coal failure characteristics play a significant role in gas occurrence states during the recovery of a working face at highly gassy coal seams. Mining-induced stress, ultrasonic wave velocity, gas pressure, and gas flow were measured to explore the relationship between coal failure characteristics and gas occurrence states. The change laws of gas occurrence states with coal failure characteristics were analyzed, and the evolutionary mechanism of gas pressure was discussed. The following conclusions are mainly drawn:

(1) The mining-induced stress, gas pressure, and gas flow are first steady, then increased, and finally reduced with the advancement of the working face; meanwhile, the ultrasonic wave velocity is first steady, then reduced, and finally steady again.

(2) The coal mass in front of the working face can be divided into intense damage, damage, and slight damage zones, outward from the rib to the coal seam strike. The gas pressure is low in the intense damage zone, maximum in the damage zone, and gradually reduced to a low value outward from the working face in the slight damage zone.

(3) The gas pressure of coal mass is mainly controlled by two basic variables: porous medium-confined gas content and porosity. The porosity of coal mass is small in the damage zone, and a large amount of gas is desorbed by internal microcracks, which is the essential cause for the elevated gas pressure. Gas treatment measures can effectively prevent and control coal and gas dynamic disasters if implemented by field technicians.

The influencing laws of failure characteristics at highly gassy coal seams in gas occurrence states were investigated through field measurement and theoretical analysis, thus providing a theoretical basis for effectively preventing and controlling coal and gas dynamic disasters. However, the coal failure characteristics were only characterized via ultrasonic wave velocity. Other detection means (acoustic emission and CT) should be combined to comprehensively analyze the gas occurrence states in coal masses with different failure degrees.

**Acknowledgements**

This work was supported by the National Natural Science Foundation of China (No.52004007), the Foundation of Educational Commission of Anhui Province (KJ2019A0130), and the Independent Research Foundation of the State Key Laboratory of Mining Response and Disaster Prevention and Control in Deep Coal Mines (SKLMRDPC19ZZ09).



## References

1. Zhang J., Xu K., Reniers G., You G. "Statistical analysis the characteristics of extraordinarily severe coal mine accidents (ESCMAs) in China from 1950 to 2018". *Process Safety and Environmental Protection*. 133(1), 2019, pp.332-340.
2. Erdogan H. H., Duzgun H. S., Selcuk-Kestel A.S. "Quantitative hazard assessment for Zonguldak Coal Basin underground mines". *International Journal of Mining Science and Technology*, 29(3), 2019, pp. 453-467.
3. Suman S. C., Pathak P. "Anjan hill mine explosion: human failures resulting 14 fatalities". *Journal of Mines, Metals & Fuels*, 66(3), 2018, pp.187-193.
4. Lu, Z. L., Zhu, X. D., Wang H.L., Li, Q. "Mathematical modeling for intelligent prediction of gas accident number in Chinese coal mines in recent years". *Journal of Intelligent & Fuzzy Systems*, 35(3), 2018, pp.2649-2655.
5. Dennis, B. J. "Review of coal and gas outburst in australian underground coal mines". *International Journal of Mining Science and Technology*, 29(6), 2019, pp. 4-13.
6. Odintsev, V. N., Shipovskii, I. E. "Simulating explosive effect on gas-dynamic state of outburst hazardous coal band". *Journal of Mining Science*, 55(4), 2019, pp.556-566.
7. Yuan L. "Theory and practice of integrated coal production and gas extraction". *International Journal of Coal Science & Technology*,2(1), 2015, pp.3-11.
8. Dvorácek, J., Hudecek, V., Šterba, J. "Economic assessment of safety measures against coal and gas outburst". *Journal of Mines, Metals and Fuels*, 61(9-10), 2013, pp.291-294.
9. Singh A. K., Sahu J. N. "Coal mine gas: a new fuel utilization technique for India". *International Journal of Green Energy*, 15(11-15), 2018, pp.732- 743.
10. Black, D. J. "Review of coal and gas outburst in Australian underground coal mines". *International Journal of Mining Science and Technology*, 29(6), 2019, pp.815-824.
11. Sobczyk J. "A comparison of the influence of adsorbed gases on gas stresses leading to coal and gas outburst". *Fuel*, 115(7), 2014, pp. 288-294.
12. Alekseev A. D., Feldman E. P., Kalugina N.A. "Thermodynamics of a gas-coal massif and a nonuniform gas distribution in a coal bed". *Technical Physics*,55(12), 2010, pp. 1766-1770.
13. Adel T., Farhang S., Faramarz D. A., Ali M. "Simulation of macerals effects on methane emission during gas drainage in coal mines".*Fuel*,210(9), 2017, pp.659 -665.
14. Si G., Belle B. "Performance analysis of vertical goaf gas drainage holes using gas indicators in Australian coal mines". *International Journal of Coal Geology*, 216(10), 2019, pp.1-15.
15. Ripepi N., Louk K., Amante J., Schlosser C.,Tang X., Gilliland E. "Determining coalbed methane production and composition from individual stacked coal seams in a multi-zone completed gas well". *Energies*,10(10), 2017, pp.1-8.
16. Lin B. Q., Liu T., Yang W. "Solid-gascoupling model for coal seams based on dynamic diffusion and its application". *Journal of China University of Mining&Technology*, 47(1), 2018, pp.32-39,112.
17. Wang Q. F., Li C.W., Zhao Y. C., Ai D. H. "Study of gas emission law at the heading face in a coal-mine tunnel based on the lattice boltzmann method". *Energy Science & Engineering*, 8(5), 2020, pp. 1705-1715.
18. Ma H.F. "Reconstruction of three-dimensional gas pressure field of mining coal seam based on matlab and measured data". *Chinese Journal of Rock Mechanics and Engineering*, 35(S1), 2016, pp.3036-3041.
19. Scott A. R. "Hydrogeologic factors affecting gas content distribution in coal beds". *Interational Journal of Coal Geology*, 2002, pp.50(1), 363-387.
20. Si L. L., Li Z. H., Yang Y. L., Xin L., Liu Z., Liu Y. A., Zhang X. Y. "Experimental investigation for pore structure and $CH_4$ release characteristics of coal during pulverization process". *Energy & Fuels*, 31(12), 2017, pp. 14357-14366.
21. Jing Y., Rabbani A., Armstrong R.T., Wang J.J., Mostaghimi P. "A hybrid fracture-micropore network model for multiphysics gas flow in coal". *Fuel*, 281(11), 2020, pp.1-11.
22. UI'yanova, E. V., Malinnikova, O. N., Burchak, A. V., Balalaev, A.K. "Gas content and structure of coal in Donets Basin". *Journal of Mining Science*, 53(4), 2018, pp. 655-662.
23. Kozyreva E.N.,Nepeina E.S. "Influence of inert-gas pressure on the sorptional methane capacity of Kuznetsk Basin coking coal". *Coke and Chemistry*, 61(9), 2018, pp.360-363.
24. Duan M., Jiang C. B., Gan Q., Zhao H. B.,Yang Y., Li Z. K. "Study on permeability anisotropy of bedded coal under true triaxial stress and its application". *Transport in Porous Media*,131(3), 2020, pp.1007-1035.
25. Xie G. X.,Hu Z. X.,Wang L. "The coupling effect of the coal seam gas pressure and mining stress in working face". *Journal of China Coal Society*, 39 (6), 2014, pp.1089-1093.

26. Wei C. H., Zhu W. C., Bai Y.,Gai D. "Numerical simulation on methane distribution legularity in deep coal seam under variable temperatures". *Journal of Northeastern University (Natural Science)*, 36 (7), 2015, pp.1033-1036.
27. Yu Q. X. "*Gas Prevention*". Xuzhou: China University of Mining and Technology Press, China, 1992, pp.11-13.